International Journal of Fatigue xxx (2014) xxx–xxx

Contents lists available at ScienceDirect

International Journal of Fatigue

journal homepage: www.elsevier.com/locate/ijfatigue

New cycle counting method for multiaxial fatigue

Vitor Anes, Luis Reis *, Bin Li, M. de Freitas

ICEMS & Dept. of Mechanical Engineering, Instituto Superior Técnico, Av. Rovisco Pais, 1049-001 Lisboa, Portugal

ARTICLE INFO

Article history:
Received 10 October 2013
Received in revised form 12 January 2014
Accepted 7 February 2014
Available online xxxx

Keywords:
Fatigue
Multiaxial loading paths
Cycle counting
Fatigue life
Damage accumulation

ABSTRACT

Multiaxial fatigue is a very important physical phenomenon in several mechanical components. Fatigue life study under cyclic stresses is of utmost importance to avoid unexpected failure of equipments, vehicles or structures. Among several fatigue characterization tools, a correct definition of a loading cycle under multiaxial fatigue loading conditions shows to be crucial to estimate multiaxial fatigue life.

The aim of this work is to achieve a correct definition for a multiaxial fatigue loading cycle and accomplish a multiaxial fatigue model to estimate block's fatigue life under multiaxial loading conditions. To reach this goal, several loading paths were carried out using the 42CrMo4 low alloy steel under different loading conditions. Sequential, proportional, non-proportional and asynchronous loading effects were modulated through eleven loading blocks. Furthermore, two models were proposed: a cycle counting method and a fatigue life evaluation criterion. The results from the proposed models were correlated with the fatigue data and compared with two well known cycle counting models: the Bannantine and Socie and the Wang and Brown criteria. The proposed models were successfully validated by experimental data. Results show that the new proposals lead to an improved multiaxial fatigue characterization under complex loading conditions.

© 2014 Elsevier Ltd. All rights reserved.

1. Introduction

In simple fatigue loading cases the cycle definition using an equivalent stress is very prompt and the inherent fatigue life correlations provides acceptable results. However, in complex loading histories, the fatigue life estimations under equivalent stress approaches, most of the times, are not in agreement with experimental data. Equivalent stress approaches are unsuitable to characterize directly the block's fatigue damage, because they yield non-conservative fatigue live estimations. In other words, the loading block's fatigue damage is greater than the one estimated by the greatest equivalent stress found in that same loading block.

Therefore, block's fatigue damage characterization must consider what happens during the entire block's loading history. Multiaxial cumulative damage is commonly calculated using the Miner's rule, or its different versions, as is used in uniaxial loading conditions.

In addition, Miner's rule considers a damage parameter in association with a cycle counting method [1]. Damage parameters must capture the physical fatigue behavior to allow considering the cumulative damage as a cycle damage summation [2–5]. Equivalent damage parameters, such as equivalent stress, keep the time relation between multiaxial load components, which is a plus, but they have some shortcomings. For instance, time histories of an equivalent stress are always positive and due to that, their time history is unsuitable to capture the whole physical damage process.

The load sign of multiaxial load components is essential information because it identifies a different damage behavior. For instance, compression and tension stress states have negative and positive sign and distinct fatigue damage behaviors. Compression stresses tend to slow down the fatigue damage and the tension ones tend to speed up the damage process. Moreover, SN damage curves are established based on a pair of positive and negative reversals i.e. a tension and compression load pair. Each uniaxial reversal contributes in a different way to the SN unitary damage composed by the compression/tension damage pair, in the case of an axial SN curve.

Therefore, a rainflow cycle counting over the time variation of an equivalent stress does not capture whole the fatigue damage behavior [6,7].

Nowadays, new approaches on cycle counting are very few [5–10]. Well-known cycle counting methods use the rainflow method or its variants. They have acceptable results under uniaxial loadings, but under multiaxial loading conditions the fatigue life estimations yields poor results. Some cycle counting criteria are

---

* Corresponding author. Tel.: +351 21 8417481; fax: +351 218417915.
E-mail addresses: vitor.anes@ist.utl.pt (V. Anes), luis.g.reis@ist.utl.pt (L. Reis), bli@ist.utl.pt (B. Li), mfreitas@dem.ist.utl.pt (M. de Freitas).

http://dx.doi.org/10.1016/j.ijfatigue.2014.02.010
0142-1123/© 2014 Elsevier Ltd. All rights reserved.

critical plane based methods, they use the rainflow method applied to the stress/strain time variation, on each projection plane, to account loading reversals. For instance, Bannantine and Socie (BS) proposed a cycle counting criterion that accounts the number of loading reversals, in the critical plane, through a rainflow routine [11].

Subsequently, a damage parameter is determined, at each reversal, using a critical plane model according to the axial or shear based damage approaches. BS method has some shortcomings in damage characterization, because the contribution of the axial and shear loading components to the fatigue damage are disconnectedly computed. Therefore, the time relation between shear and axial load components is ignored, and the joint damage effect is not captured. Wang and Brown (WB) [2] proposed a new cycle counting method to overcome the sign lost shortcoming in their equivalent strain approach. WB cycle counting criterion is based in the von Mises relative strains and in the classic rainflow cycle counting method.

The loading cycles are extracted from the von Mises relative strain time variation and the WB damage parameter is computed for every extracted cycle. Then, an accumulated criterion must be used to calculate the loading block's total damage in order to estimate block's fatigue life. The WB criterion has one main shortcoming, which is the possibility to miss the greatest stress range during the loading time history [12,13].

Meggiolaro and de Castro, proposed one modification to the Wang and Brown criterion to overcome this shortcoming. The change was to expand the WB criterion to the five-dimensional Euclidean space to ensure that the highest relative strain amplitude is always accounted [6,7]. Wei and Dong proposed an equivalent stress cycle counting method using the time evolution of the equivalent stress in the von Mises stress space. The equivalent stress is mapped to extract loading cycles and overcome the missing loading path-dependency verified on the WB criterion [12–14].

In this paper is studied eleven loading blocks with several different loading effects using the Bannantine and Socie, Wang and Brown and a new proposed multiaxial cycle counting method. The new cycle counting method, the Stress Scale Factor (SSF) virtual cycle counting, is based on the SSF equivalent shear stress early proposed by the authors in [15].

Moreover, a new criterion to evaluate fatigue life under complex loadings is proposed, this method uses the new cycle counting method proposed here and is an update of the SSF equivalent shear stress to block loading conditions.

In order to validate the proposed methods it was performed a fatigue life correlation using fatigue data from eleven loading blocks. Moreover, the proposed models estimations were compared with two state-of-the-art models estimations in this field. Results show that the proposed cycle counting and fatigue life estimation approaches yields better results. In addition, the proposed models computational work is far less than the one necessary in BS and WB fatigue life evaluation.

2. Theoretical development

To estimate fatigue lives from loading blocks is necessary to consider a multidisciplinary approach in fatigue damage characterization. Multiaxial block loadings have much more intricate loading histories than the reference ones used to set up SN curves. To achieve block loading damage is necessary to enter with three main fatigue approaches: a cycle counting method, a damage criterion and a damage accumulation model. The damage criterion is the base stone to set up random fatigue. The damage parameter must capture the fatigue damage behavior to allow set up a cycle counting method and an accumulation model.

2.1. Multiaxial cycle counting

Uniaxial cycle counting is a well-understood matter. Hysteresis analysis to find a load cycle is a method that has proved to be reliable in uniaxial fatigue damage characterization. However, under multiaxial loading conditions such prompt method does not exist. Efforts has been done to adapt the uniaxial cycle counting method to the multiaxial loading histories [16–19]. BS and WB cycle counting methods are an example of that; they use the rainflow paradigm to extract the loading cycles within a multiaxial loading history.

2.2. Bannantine and Socie (BS)

Bannantine and Socie [2] proposed a multiaxial cumulative damage criterion based on a mix of critical plane damage parameter, rainflow cycle counting method and Miner's rule. The main concept behind BS criterion is based on the experimental evidence that some materials are more sensitive to axial strains than to shear strains and vice versa.

Therefore, authors concluded that the axial and shear strains have different damage scales in the same material. Bannantine and Socie considered that the block damage under multiaxial loading conditions could be estimated through axial strains or shear strains.

Thus, the criterion of choice is based on the material sensitivity to axial or shear damage. To evaluate complex loadings Bannantine and Socie proposed that the multiaxial axial and shear strains components could be treated as uniaxial loads in the critical plane search. Therefore, the multiaxial loading is projected into the candidate plane, and then the in-plane and normal strains are separately computed with a rainflow method.

After that the axial and shear accumulated damage is calculated for each plane. The plane with the highest accumulated damage is the critical plane. BS approach states that the rainflow cycle counting on each plane can be associated with the hysteresis loops in that same plane. The BS approach uses the original main paradigm behind the rainflow cycle counting methodology [11,20–22] to capture the critical plane damage. The damage accumulation at each plane is accounted through any cumulative damage model. The most used is the Miner's rule, where is performed by a linear summation of each loading cycle damage. Several accumulative damage approaches based on the Miner's rule can be found in literature [1,23]; they are mainly a non-linear versions of the Miner's original law. In the authors' opinion, the non-linearity in damage accumulation must be left to the damage parameter since SN curves are already non-linear. Therefore, in this study the linear Miner's rule is adopted. The BS damage parameter is determined based on a specific critical plane criterion. For instance, if the axial strains are cycle counted, then a critical plane model based on normal strains must be considered. Likewise, if the in-plane strains (shear strains) are cycle counted then a critical plane based in shear strains must be considered. For example, reversals damage can be accounted using Eq. (1) in shear strains and in axial strains can be used Eq. (2).

Fatemi–Socie (F–Socie) damage parameter:

$$\max_{\theta}\left\{\frac{\Delta\gamma_{\max}}{2}\cdot\left(1+k\cdot\frac{\sigma_{n,\max}}{\sigma_y}\right)\right\}=\frac{\tau_f'}{G}(2N_f)^{b\gamma}+\gamma_f'(2N_f)^{c\gamma} \tag{1}$$

where $\Delta\gamma_{\max}/2$ is the maximum shear strain amplitude on a θ plane, $\sigma_{n,\max}$ is the maximum normal stress on that plane, σ_y is the material monotonic yield strength and k is a material constant, $k = 1.0$ in this case. G is the Shear modulus, $2N_f$ is the fatigue life and τ_f', b, γ_f', γ and c are material's constants (cyclic properties).

SWT damage parameter:

Please cite this article in press as: Anes V et al. New cycle counting method for multiaxial fatigue. Int J Fatigue (2014), http://dx.doi.org/10.1016/j.ijfatigue.2014.02.010

$$\max_{\theta}\left\{\sigma_{n,\max}\cdot\frac{\Delta\varepsilon_1}{2}\right\}=\frac{\sigma_f'^2}{E}(2N_f)^{2b}+\sigma_f'^2\varepsilon'(2N_f)^{b+c} \tag{2}$$

where σ_n is the normal stress on a plane θ, and $\Delta\varepsilon_1$ is the principal strain range on that plane. E is the Young's modulus, $2N_f$ is the fatigue life and τ_f', b, ε' and c are material's constants (cyclic properties). Socie and Marquis [2], suggests that the damage within a block loading can be estimated by adding in each candidate plane the damage from normal and shear strains. The main idea is to get the total fatigue damage through a combination of two different damage behaviors. Eq. (3) presents this idea, where the largest fatigue damage occurs in the plane with the smallest value of $N(\theta)$, (i.e. the critical plane).

$$\frac{1}{N(\theta)}=\frac{1}{N_\sigma(\theta)}+\frac{1}{N_\tau(\theta)} \tag{3}$$

$N_\sigma(\theta)$ and $N_\tau(\theta)$ are the fatigue life estimations obtained through a critical plane based on axial and shear strains, respectively. The Socie and Marquis approach aforementioned has one main shortcoming because it considers twice the same axial damage contribution. In fact, if the total fatigue damage is accounted based on Fatemi–Socie and SWT damage criteria, one fraction of axial damage is double counted. This is so because F–Socie criterion corrects the shear strain amplitude with the greatest axial stress. Usually, the critical plane criteria adopt the highest damage parameter to estimate fatigue lives. However, there are differences between the highest damage and the highest accumulated damage in fatigue life estimations. The highest damage parameter considers just the load reversal with the highest amplitude within a loading block, at a specific plane. Therefore, damage from other reversals is not accounted, but in accumulated damage criteria every reversal in a specific plane is accounted. In order to check the BS criterion in this study, the block damage is accounted by identifying the critical plane with the highest accumulated damage based on shear or normal strains. Moreover, was adopted here the ASTM rainflow cycle counting criterion and the Miner's rule to achieve the total fatigue damage at a specific plane.

Fig. 1 shows the Bannatine and Socie method to estimate a block fatigue life.

2.3. Wang and Brown

Wang and Brown [24] proposed a multiaxial cycle counting model where reversals within a loading block are extracted through the von Mises equivalent strain/stress. This approach just identifies the region from the loading path that belongs to each reversal.

A damage parameter can be applied to each one of the reversals identified as if it were a new and unique loading path. The von Mises equivalent strain/stress has attached the loading sign loss shortcoming i.e. the equivalent strain/stress is always positive regardless compression, tension or shear directions.

This is an important matter because completely reversed load is transformed into a zero to maximum creating a virtual mean stress on the loading path that does not exist.

In order to avoid this shortcoming Wang and Brown have proposed to make a rainflow cycle counting to the relative von Mises strains. To extract the reversals within a loading block, the multiaxial loading history is calculated to get the von Mises equivalent strain time evolution. After that, the maximum equivalent strain location is identified to move the time origin to that same location. Identifying the maximum equivalent strain location is the preliminary modus operandi to carry out the Wang and Brown cycle counting method. The time evolution of the relative equivalent strain is then calculated by computing the norm between the instantaneous equivalent strain and the maximum equivalent strain value. After that, a rainflow cycle counting is performed into the relative equivalent strain time evolution. Later, the reversal is extracted and the relative equivalent strain history is updated by removing the information inherent to that same cycle. The remaining loading history is computed in the same way until finish all available loading branches.

A map is obtained with the WB method; it splits the loading path into loading regions i.e. loading reversals. For each reversal a critical plane search is performed to find out the damage parameter inherent to that cycle.

Eq. (4) shows the Brown Miller critical plane criterion typically used with the Wang and Brown cycle counting method.

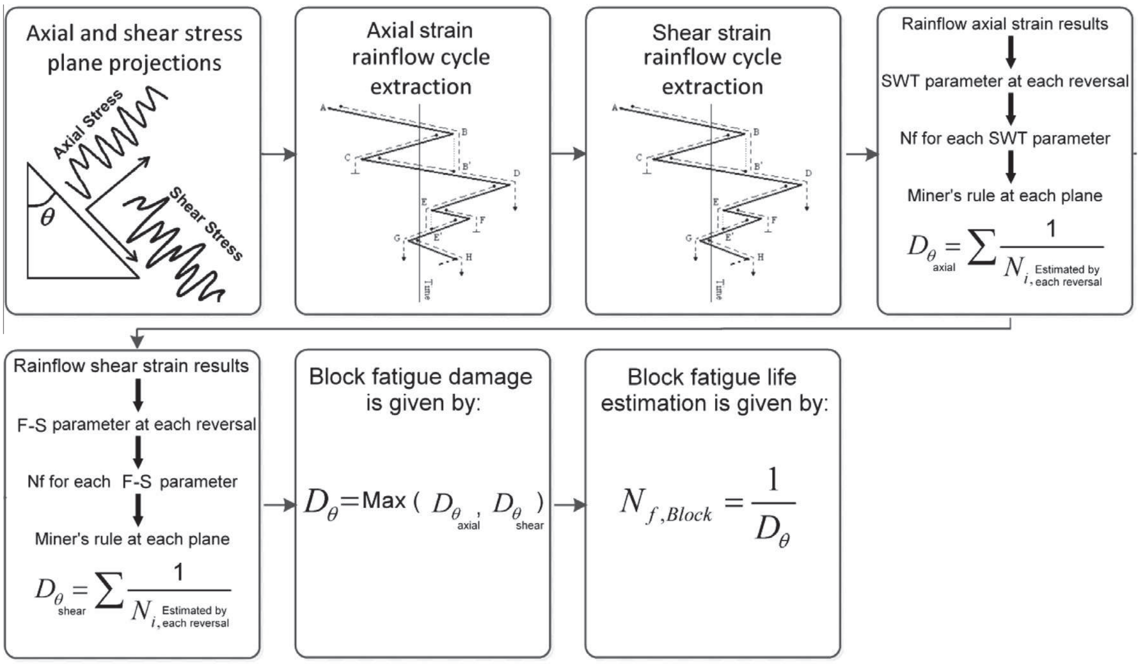
Axial and shear stress plane projections
Axial Stress
Shear Stress
θ
Axial strain rainflow cycle extraction
Shear strain rainflow cycle extraction
A
B
B'
C
D
E
E'
F
G
H
Time
Rainflow axial strain results
SWT parameter at each reversal
Nf for each SWT parameter
Miner's rule at each plane
$D_{\theta_{\text{axial}}}=\sum\frac{1}{N_{i,\text{Estimated by each reversal}}}$
Rainflow shear strain results
F-S parameter at each reversal
Nf for each F-S parameter
Miner's rule at each plane
$D_{\theta_{\text{shear}}}=\sum\frac{1}{N_{i,\text{Estimated by each reversal}}}$
Block fatigue damage is given by:
$D_\theta=\text{Max}\,(D_{\theta_{\text{axial}}},D_{\theta_{\text{shear}}})$
Block fatigue life estimation is given by:
$N_{f,Block}=\frac{1}{D_\theta}$

Fig. 1. Bannantine and Socie methodology.

$$\varepsilon = \frac{0.5(\Delta\gamma_{\max}) + S(\delta\varepsilon_n)}{1+\nu'+(1+\nu')S} = \frac{\sigma'_f - 2\sigma_{n,mean}}{E}(2N_f)^b + \varepsilon'_f(2N_f)^c \quad (4)$$

where $\Delta\gamma_{\max}$ and $\delta\varepsilon_n$ are the shear strain range and the normal strain excursion between two turning points of shear strain computed on the maximum shear strain plane. The S parameter near fatigue limit is equal to 0.3, for half fatigue life S takes the value 0.7, [2].

E is the Young's modulus, $\sigma_{n,mean}$ is the mean normal stress within the loading path, $2N_f$ is the fatigue life and τ'_f, b, ε' and c are material's constants (cyclic properties).

Subsequently, a cumulative damage criterion must be used to account the block damage to estimate the inherent fatigue life [24]. Fig. 2 shows an example of the Wang and Brown method where it is found out the reversals within a loading block. Fig. 2a shows the axial and shear loading components time evolution. Afterwards the von Mises strain/strain time evolution is computed see Fig. 2b. Next step is to find the first von Mises strain/strain maximum value and translate the graph origin to that point. In Fig. 2c is shown the referential translation for the first maximum von Mises equivalent stress named as point A.

At this point the relative von Mises time history ($\sigma_{i,relative}$) is determined by subtracting, in the translated loading path, the axial and shear components at origin. Eq. (5) shows the numeric method to get the relative time history. As a result, the relative von Mises time histories always start at zero.

$$\sigma_{i,relative}(t) = \sqrt{(\sigma_i(t) - \sigma_{\max})^2 + 3\cdot(\tau_i(t) - \tau_{\max})^2} \quad (5)$$

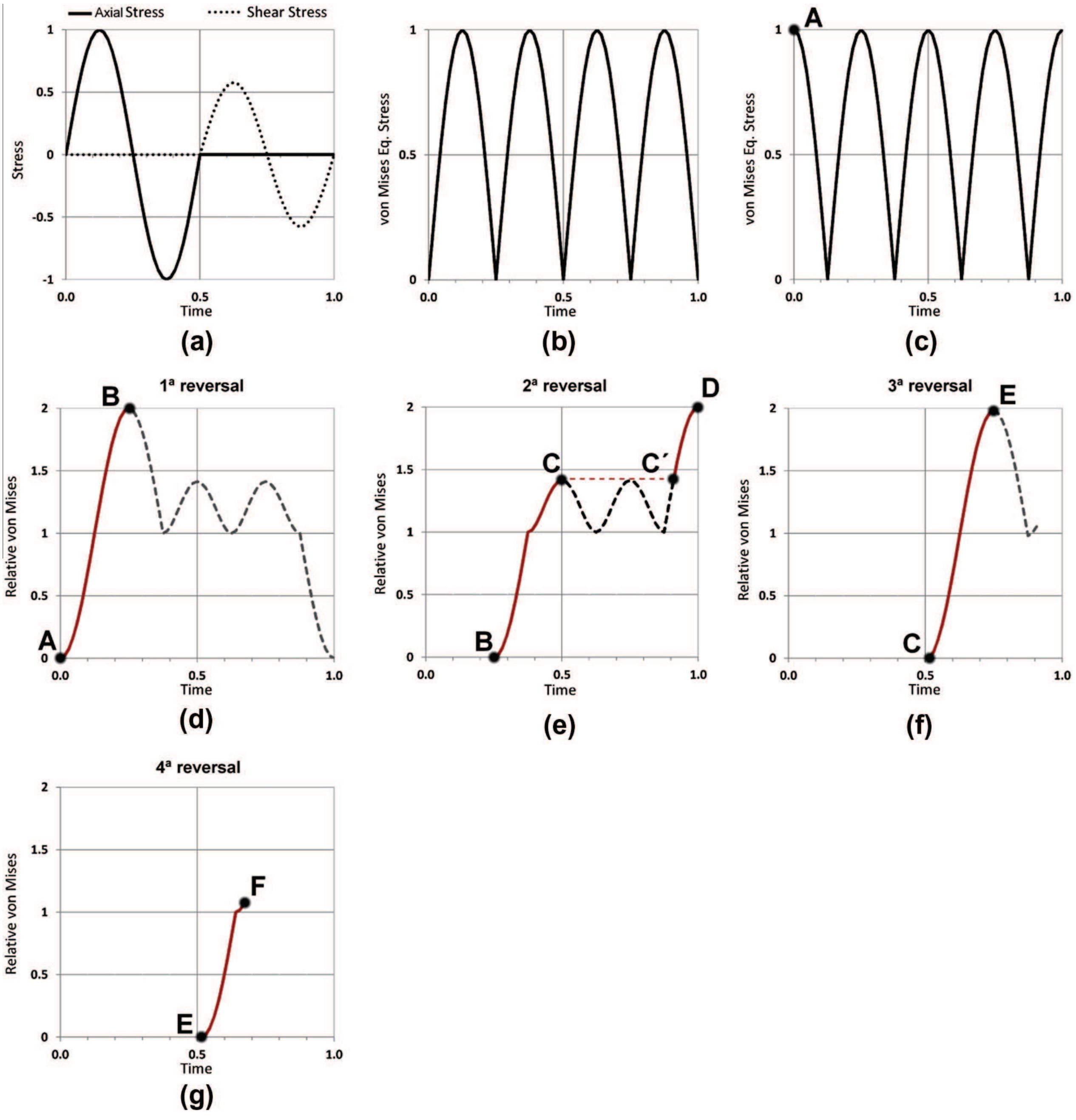

Fig. 2. Wang and Brown reversal extraction example.

Please cite this article in press as: Anes V et al. New cycle counting method for multiaxial fatigue. Int J Fatigue (2014), http://dx.doi.org/10.1016/j.ijfatigue.2014.02.010

where σ_i and τ_i are the instantaneous axial and shear stresses, respectively. $\sigma_{\max}$ and $\tau_{\max}$ are the maximum axial and shear stresses found within the loading history.

To extract a reversal it is selected on the relative von Mises time history the loading path branch that starts to increase from zero. When the relative time history starts to decrease, the reversal extraction goes on the horizontal until the time history starts again to increase. If the horizontal extraction does not find any increasing relative time history branch, then the reversal ends at the point where the extraction initiates to become horizontal.

Fig. 2d shows the 1ª reversal extraction represented by line AB; at this stage, no highest point than point B is found, so the reversal was extracted. Later, the axial and shear components inherent to the reversal extracted must be removed from the loading block path. Then the procedure starts again with the updated axial and shear stress loading path; just one reversal is extracted for each one relative time history. In Fig. 2e is shown that point B is the new relative minimum. Continuing the reversal extraction process it is achieved point C; at this point the von Mises time history decreases, then the dot line goes straight to find the point C′.

The reversal extraction continues to the time history end. The second reversal was extracted with the points BCC′D. Then the axial and shear stress loading paths are updated again. The new von Mises relative minimum is located at point C from where grows until it reaches point E, being extracted the 3rd reversal, CE, see Fig. 2f.

Next, the axial and shear stress is updated by removing the reversal CE axial and shear components from the original loading path. After that the new relative von Mises time evolution is calculated, see Fig. 2g.

The reversal extraction starts at point E and increases to reach point F. At this stage, entire loading path was updated and it was found every reversal within the loading block. In this example, the loading block time history was separated in four sections, i.e. four reversals.

2.3.1. Wang and Brown block fatigue life estimation

Each one of the achieved sub-loading paths (reversal zones) must be considered as independent loading paths. Then, for each reversal, the damage criterion must be calculated and the inherent fatigue life estimated.

Afterwards, Miner's rule is used to compute the block accumulated damage and the block fatigue life can be estimated, using Eq. (6):

$$D_{block} = \sum_{i=1}^{\#reversals} \frac{1}{N_{f\_i}} \tag{6}$$

where N_{f_i} is the reversal fatigue life estimation and D_{block} is the total damage within a loading block. Thus, the block fatigue life can be estimated as follows, Eq. (7):

$$N_{block} = \frac{1}{D_{block}} \tag{7}$$

where N_{block} is the block fatigue life estimation.

2.4. New cycle counting and block's fatigue life evaluation criterion

Authors propose here a new criterion to estimate loading block's fatigue life. Moreover, a new cycle counting method to account loading block's fatigue damage is also proposed, i.e. a non-rainflow cycle counting method based on the SSF equivalent shear stress is presented. In the author's opinion, equivalent stress approaches are suitable to account block's fatigue damage. Equivalent stress criteria packed in one damage parameter the instantaneous damage contributions of axial and shear loadings, which is a huge advantage.

2.4.1. SSF equivalent stress approach

The SSF equivalent stress approach was carried out by the authors [15]. The proposed approach considers that the stress amplitude ratio and the stress loading level have a huge influence in the material fatigue strength. These influences were accounted through the SSF function that transforms an axial damage into a shear one. With the SSF equivalent shear stress it is possible to estimate fatigue lives using Eq. (8).

$$\max_{block}(\tau + ssf \cdot \sigma) = A(N_f)^b \tag{8}$$

where τ and σ are the instantaneous load components, A and b are the power law trend line components of the torsional fatigue life results (torsion SN curve), and N_f is the fatigue strength under certain stress level. The SSF function is given in Eq. (9):

$$ssf(\sigma,\lambda) = a + b \cdot \sigma + c \cdot \sigma^2 + d \cdot \sigma^3 + f \cdot \lambda^2 + g \cdot \lambda^3 + h \cdot \lambda^4 + i \cdot \lambda^5 \tag{9}$$

where σ is the axial component of the biaxial loading and $\lambda = \tau/\sigma$ is the stress amplitude ratio. Constants from "a" to "i" are determined through experimental tests. The SSF function is a material fatigue property and must be determined by experimental tests [15].

2.4.2. SSF virtual cycle counting

Cycle counting methods are used in fatigue life evaluation because the maximum damage parameter within a loading block does not capture the block's fatigue damage. Therefore, block's fatigue life estimations obtained solely with a maximum damage parameter yields poor results. Here it is presented the SSF virtual cycle counting method. In this new approach are not analyzed hysteresis loops and due to that it was named as virtual cycle counting. However, the new method is physically based. It relates the maximum damage parameter, within a loading block, with the block's total damage.

Fig. 3 shows the SSF virtual cycle counting method in association with the block's fatigue life estimation method. Fig. 3a presents the axial and shear stress components time variation of a multiaxial loading which are computed to get the SSF time history, see Fig. 3b. Next, in Fig. 3c is selected, from the SSF time history, the highest SSF value and the SSF stress value at every peak and valley found between two consecutive SSF zero stress points.

The highest SSF value is the block's damage reference to achieve the block's damage, see Fig. 3d and e. The virtual cycle counting is achieved by adding each SSF peak/valley absolute values and dividing the result by the block's damage reference. Eq. (10) shows the virtual cycle counting expression.

$$vcc = \frac{\sum abs(\tau)_{peak,valley}}{2 \cdot \tau_{\max,Block}} \tag{10}$$

where vcc is the virtual cycle count inherent to a loading block and τ is the SSF equivalent shear stress at each peak/valley. When the loading block is defined by two SSF reversals, i.e. one peak and one valley, the vcc is equal to 1. In this way SSF virtual cycle counting accounts for 1 cycle loading cases, that usually are the reference ones.

Carrying out the proposed multiaxial cycle counting method it is much easier than other cycle counting methods such as BS and WB.

Please cite this article in press as: Anes V et al. New cycle counting method for multiaxial fatigue. Int J Fatigue (2014), http://dx.doi.org/10.1016/j.ijfatigue.2014.02.010

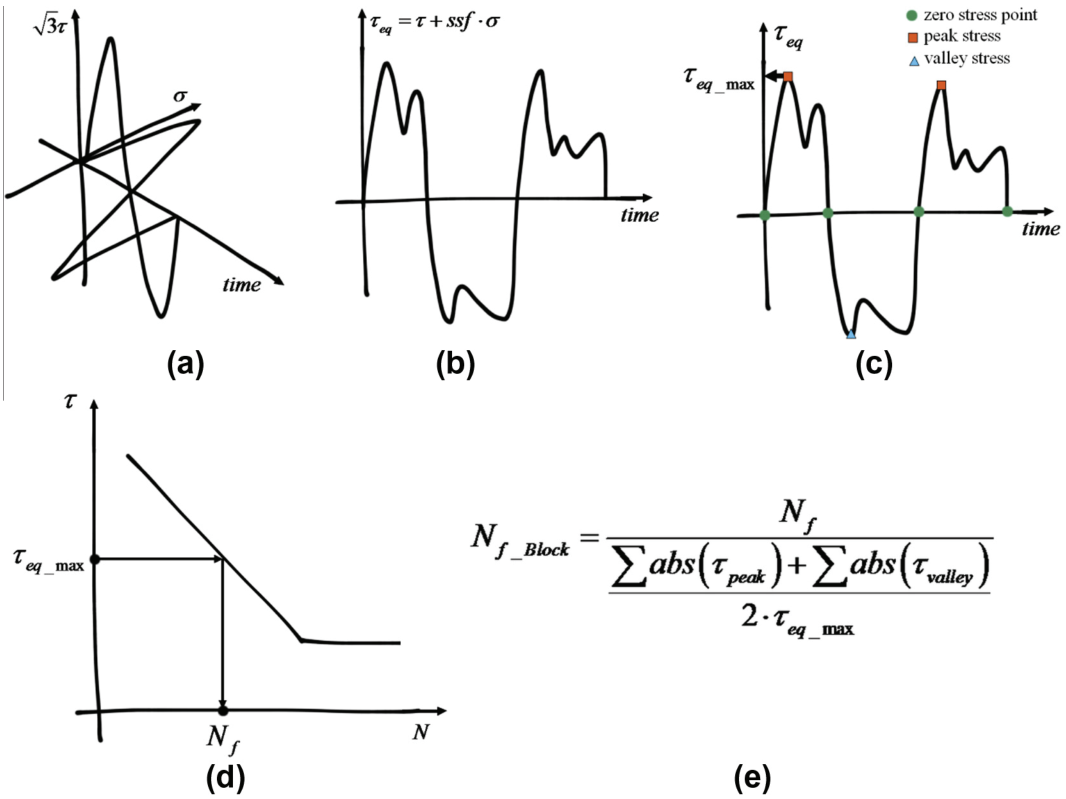

Fig. 3. SSF virtual cycle counting method and block's fatigue life estimation.

2.4.3. New block's fatigue life criterion

The block's fatigue life estimation is achieved by using the block's reference damage and the virtual cycle count as follows, Eq. (11):

$$N_{f\_block} = \frac{N_{f\_\tau\ \max}}{vcc} \tag{11}$$

where N_{f_block} is the block's fatigue life estimation and $N_{\tau\ \max}$ is the fatigue life estimation reference damage determined by Eq. (12):

$$N_{f\_\tau\ \max} = \left(\frac{\tau_{\max,Block}}{A}\right)^{\frac{1}{b}} \tag{12}$$

where A and b, are the power law regression components obtained from pure torsion fatigue data.

3. Materials and methods

3.1. Material

A 42CrMo4 quenched and tempered high strength steel was used in this work. The test specimens were machined from rods with a 25 mm diameter.

The specimen's geometric shape was a solid hourglass with a 6.35 mm diameter at middle length [15].

Specimens were inspected and manually polished using sandpapers of decreasing grain size, from P200 to P1200. Fatigue tests were carried out through a multiaxial servo-hydraulic machine under load control at room temperature.

Tests were performed under axial and torsion fully reversed conditions as shown in Fig. 4. Testing frequency was 5 Hz.

3.2. Loading blocks

To do the comparative study between the accumulated damage criteria presented in the earlier sections, eleven loading blocks were tested and analyzed.

Fig. 4 shows the loading blocks on the axial and shear stress time history evolution.

4. Results and discussion

4.1. S–N results

Table 1 shows the experimental fatigue life results for the selected loading blocks. The Axial and Shear labels, presented in Table 1, are the highest stress in axial and shear loading channels, respectively. N_f is the number of cycles to failure and (ro) is a run out test.

4.2. Theoretical cycle counting results

Theoretical cycle counting results, for the selected criteria, are presented in Figs. 5–15. For each loading block, the selected criteria and the new approach results are presented in the same figure to turn easier the comparative analysis.

4.2.1. How to interpret the results

Cycle counting results are presented here in different ways because each criterion have distinct approaches and different ways to yield the results. However, the number of cycles within each loading block is focused here as a common result between the selected criteria. In Figs. 5–15, the sub-figures (a–c) are related to each other. The loading path in sub-figure (a) is presented in the von Mises stress space, from which is analyzed the critical plane

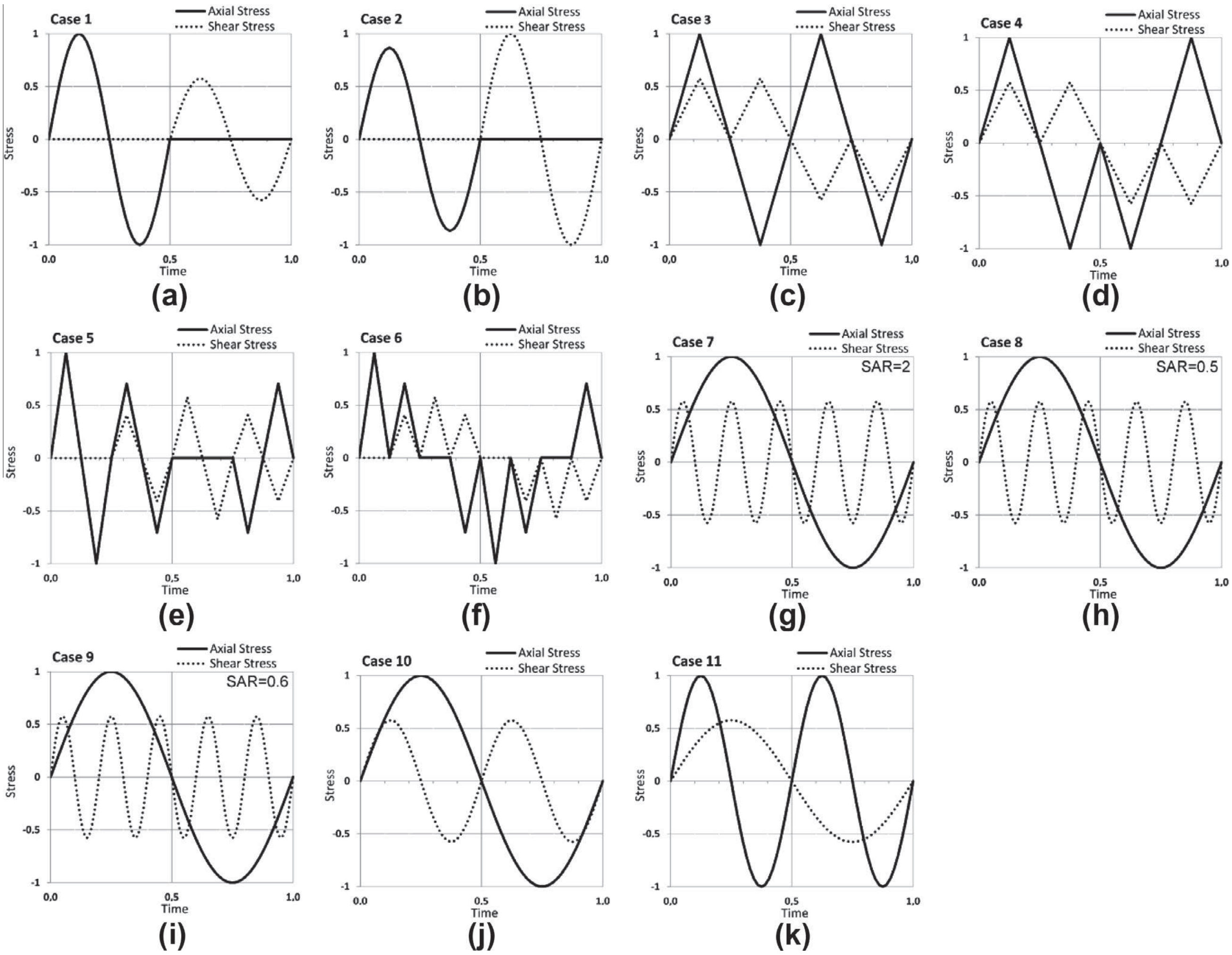

Fig. 4. Axial and shear stress time evolution of the selected loading blocks.

estimations and the loading path shape. In experiments, specimens test had their longitudinal direction lined up with the σ axis, shown in sub-figures (a), and 0° crack direction is parallel to τ axis. Bannantine and Socie results are shown in sub-figures (b and c). To estimate the loading block fatigue life the accumulated damage was determined and represented by a solid line at each loaded plane. Furthermore, a dotted line represents the BS reversals number at each loaded plane. Moreover, sub-figures (d and e) are related to each other. Sub-figure (d) shows the axial and shear stresses time variation and sub-figure (e) shows the Wang and Brown criterion results. WB reversals number is a time dependent result and the most damaging reversal occurrence can be identified in the stress–time loading history presented in sub-figure (d). Likewise, the SSF equivalent stress time variation, shown in sub-figure (f) can be compared with sub-figure (d) where it is shown the loading block stress–time variation. Furthermore, the critical plane reversals number shown in sub-figures (b and c) have a different paradigm than the WB block reversal number presented in sub-figure (e). In critical plane approach, the reversals results are related to the number of reversals computed in each plane. On the other hand, Wang and Brown reversal results show the reversal time in the loading block period.

4.2.2. Results analysis

Fig. 5 shows the results of the loading Case 1. Case 1 is a sequential loading where a sinusoidal axial load is followed by a sinusoidal shear load $\sqrt{3}$ times less than the axial one. Regarding BS results, the SWT and F–Socie criteria estimate the critical plane direction at 0° with 4 and 3 reversals, respectively. The experimental critical plane for loading Case 1 is $-5°$. Considering the critical plane estimation calculated without accumulated damage approach, the SWT and F–Socie critical plane estimations were 0° in SWT and ±90°; 0° in F–Socie. In Fig. 5b, at $-45°$ is shown that the loaded plane has 6 reversals, however the inherent damage parameter is near zero.

Moreover, the maximum damage parameter was found at 0° where the reversals number is lower than the one found at $-45°$. It shows that the number of reversals must be always kept up in association with the damage parameter. Regarding WB results it can be concluded that Case 1 has 4 reversals. The most loaded reversal is the 2nd one which is divided into two time periods, see Fig. 5e. Comparing the WB results with the block stress–time history, see Fig. 5d, it can be concluded that the most damaging period is between 16 and 33 s and from 57 to 65 s. Therefore, WB most loaded reversal, 2nd one, outcome from the axial compressive and from the last shear loading branch. SSF time variation presented in Fig. 5f is very similar to the stress–time variation presented in Fig. 5d having the zero stress points at the same time. The SSF cycle counting method extracts 3.4 reversals and the rainflow method extracts from the SSF time variation 5 reversals.

Fig. 6 presents the loading Case 2 results. Case 2 is a sequential loading block like the loading Case 1 with the particularity that the

Table 1
42CrMo4 fatigue life results.

Case	Axial	Shear	N_f
Case 1	610	352	24,722
	600	346	30,058
	570	329	58,703
	520	300	176,793
	495	286	265,955
	480	277	271,243
	445	257	892,629
	420	243	1,000,000 (ro)
Case 2	360	416	337,186
	345	398	518,622
	375	433	121,014
	305	352	1,000,000 (ro)
Case 3	450	260	21,485
	440	254	32,374
	435	251	41,060
	415	240	128,000
	405	234	181,991
	395	228	427,877
Case 4	420	243	34,807
	415	240	53,246
	410	237	86,669
	400	231	115,474
	395	228	119,252
	380	219	231,943
	370	214	282,332
Case 5	520	300	26,009
	552	318	26,509
	540	312	82,293
	520	300	461,232
	490	283	733,273
Case 6	479	240	4,088
	463	232	10,719
	434	217	37,031
	399	200	99,052
	347	173	558,219
Case 7	194	388	35,003
	184	368	47,934
	175	350	79,496
	160	321	133,058
	143	287	1,000,000 (ro)
Case 8	520	300	36,102
	493	285	76,297
	487	281	90,993
	466	270	117,530
	441	255	464,214
Case 9	470	271	38,487
	465	269	52,836
	455	263	86,000
	440	254	127,693
	430	248	265,312
	420	248	803,827
Case 10	510	294	12,116
	480	277	41,466
	460	266	93,247
	440	254	200,489
	435	251	421,814
	430	248	692,953
Case 11	440	254	32,350
	425	245	53,116
	415	240	96,837
	410	237	123,305
	405	234	158,375
	400	231	342,411

shear stress amplitude is now greater than the axial one. The SWT critical plane estimation is ±45° where the BS criterion yields 6 and 5 reversals, respectively reaching the same accumulated damage in each critical plane. F–Socie criterion estimates the critical plane at 0° from which BS yields 3 reversals.

The experimental critical plane for loading Case 2 is 0°. Considering the critical plane estimation calculated without accumulated damage approach, the SWT and F–Socie critical plane estimations were ±45° in SWT and ±90°; 0° in F–Socie. WB results are very alike to the ones verified in the loading Case 1, where the greatest damage occurs at the 2nd reversal.

The SSF time variation and the block stress–time variation have both zero stress points at the same time. SSF criterion extracts 3.6 reversals from Case 2 and rainflow criterion applied to the SSF time evolution extracts 5 reversals.

Fig. 7 shows the results for the loading Case 3, which is composed of several proportional loading branches, with different sequential loading paths, see Fig. 7a. BS extracts 7 reversals in both SWT and F–Socie critical plane criteria. SWT results show that the greatest accumulated damage occurs at ±30°, moreover for the F–Socie criterion the critical plane estimation is ±16°. The experimental critical plane for loading Case 3 is 29°.

Considering the critical plane estimation and neglecting the accumulated damage approach, the SWT and F–Socie critical plane estimations are ±25° in SWT and ±25°; ±69° in F–Socie.

WB results identify the most damaging reversal at the last loading branch and extracted 6 reversals from the loading block.

SSF accumulated damage criterion yields 4.2 reversals. The rainflow results yields 5 reversals for the SSF time variation.

Fig. 8 presents the results of loading Case 4. This loading block is similar to the loading Case 3 but with different loading sequence. Case 4 does not have a fully reversed stress–time variation likewise Case 3, see sub-figure a. BS results are presented in Figs. 8b and c. SWT and F–Socie yields the same reversals amount and the estimations to the crack initiation direction were ±29° in SWT and ±17 in F–Socie. Experimental results of loading Case 4 show the crack initiation plane occurs at 31°. The critical plane estimations without accumulative damage approach were ±25° in SWT and ±21°/±69° in F–Socie. From the results it can be concluded that the loading sequence change between Cases 3 and 4 do not affect the critical plane estimation and experimental crack initiation direction. WB yields 6 reversals, see Fig. 8e, which is the same value extracted by the BS method. WB results suggest the last reversal as the most damaging one. SSF extracts 4 reversals and the rainflow applied to the SSF time change yields 6 reversals.

Case 5 results are summarized in Fig. 9. This loading block is composed of several proportional loading branches with different stress amplitude ratios (SAR). The sequence number presented in the loading path gives the block's load sequence; see Fig. 9a. BS yields 10 reversals under SWT and F–Socie damage criteria.

The critical plane direction estimated under the BS accumulated damage approach was 4° for SWT and 0° for F–Socie. Experimental results show that crack initiation plane occurs at 0°. Critical plane results obtained without a damage accumulation approach estimates the critical plane direction at 0° in SWT and F–Socie criteria. WB method extracts 9 reversals from loading Case 5, minus 1 reversal than the ones obtained by the critical plane criteria in association with the BS approach. SSF criterion extracts 6.8 reversals and the rainflow method extracts 10 reversals from the SSF time variation.

Fig. 10 summarizes the cycle counting results of loading Case 6. Case 6 is similar to Case 5, the difference between them is related to the load sequence presented in Fig. 10a. At loading Case 6, BS yields 10 reversals for SWT and 11 reversals for F–Socie at the most loaded plane (higher damage parameter). It can be concluded from Fig. 10b and c that the critical plane is not the one that has the greatest amount of reversals.

Estimations for the critical plane directions with BS accumulated damage criterion were −2° for SWT and 0° for F–Socie. The experimental critical plane direction was −22°.

Critical plane estimations without using a damage accumulation approach were −25°; 23° in SWT and −23°; 20° F–Socie

Please cite this article in press as: Anes V et al. New cycle counting method for multiaxial fatigue. Int J Fatigue (2014), http://dx.doi.org/10.1016/j.ijfatigue.2014.02.010

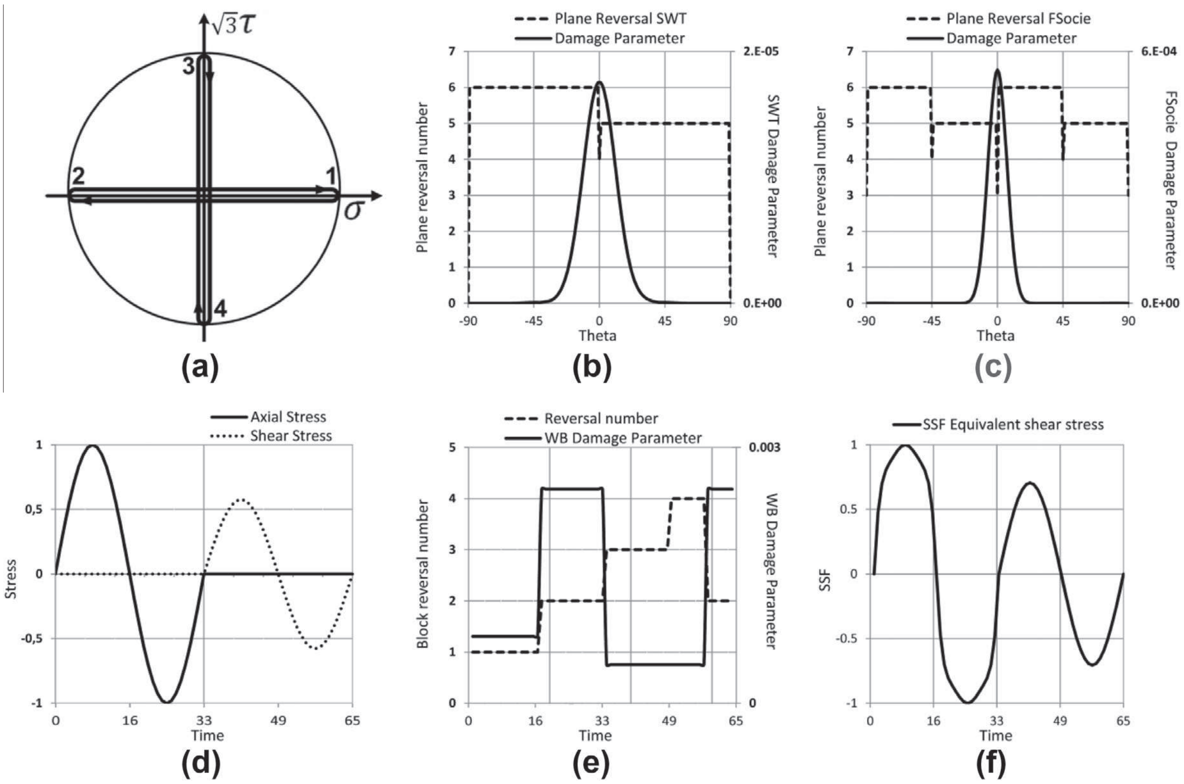

Fig. 5. Case 1: (a) von Mises stress space, (b) BS results with SWT, (c) BS results with F–Socie, (d) block stress–time change, (e) WB results and (f) SSF time change.

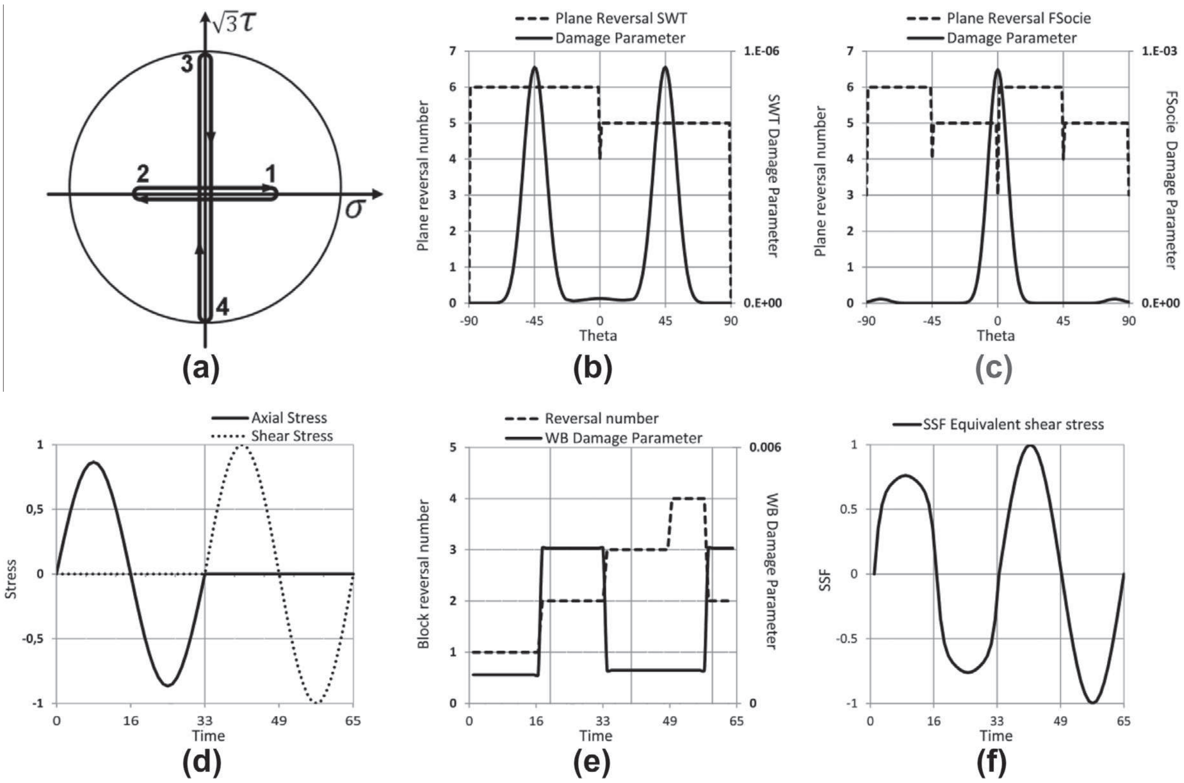

Fig. 6. Case 2: (a) von Mises stress space, (b) BS results with SWT, (c) BS results with F–Socie, (d) Block stress–time change, (e) WB results and (f) SSF time change.

criteria. WB method suggests the reversal number 8 as the most damaging one and extracts 14 reversals from the loading block. SSF method extracts 6.8 reversals and the rainflow method applied to the SSF time evolution yields 14 reversals.

Figs. 11–13 show the cycle counting results for the loading Cases 7–9, respectively. Cases 7–9 are asynchronous loading blocks, where the shear stress frequency is five times greater than the axial one. The difference between these three loading blocks is

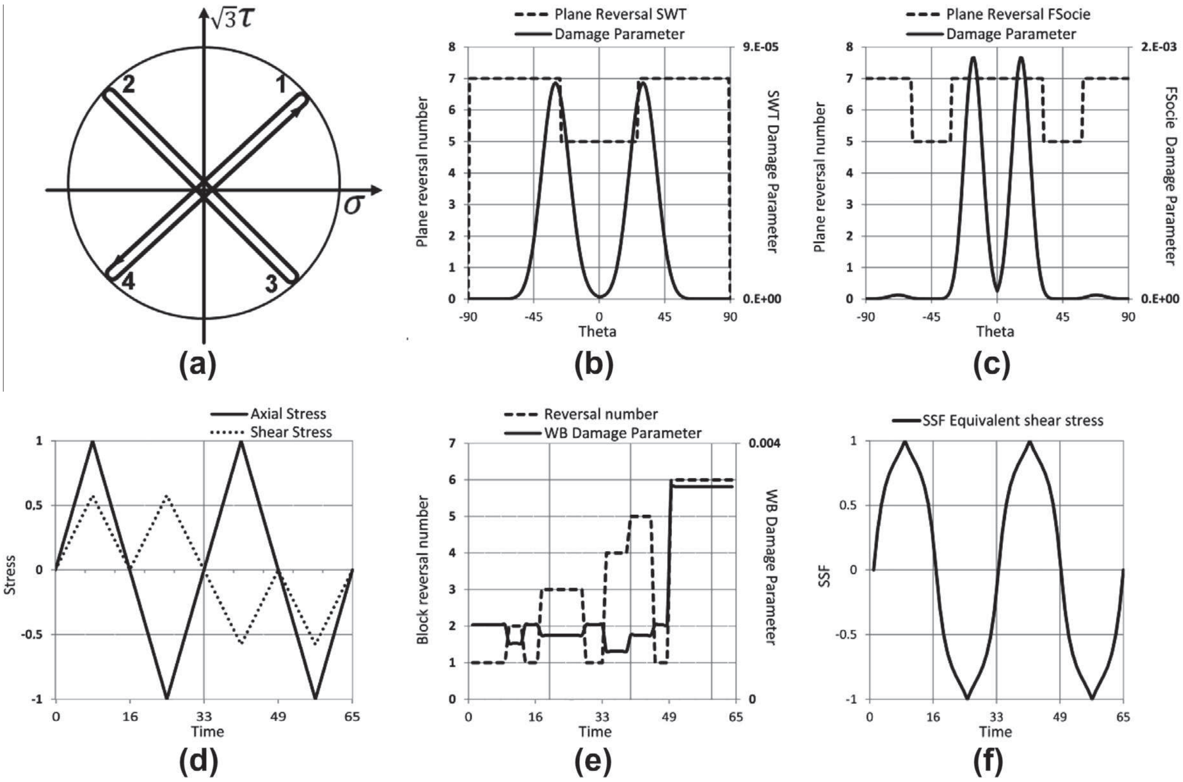

Fig. 7. Case 3: (a) von Mises stress space, (b) BS results with SWT, (c) BS results with F–Socie, (d) Block stress–time evolution, (e) WB results and (f) SSF time evolution.

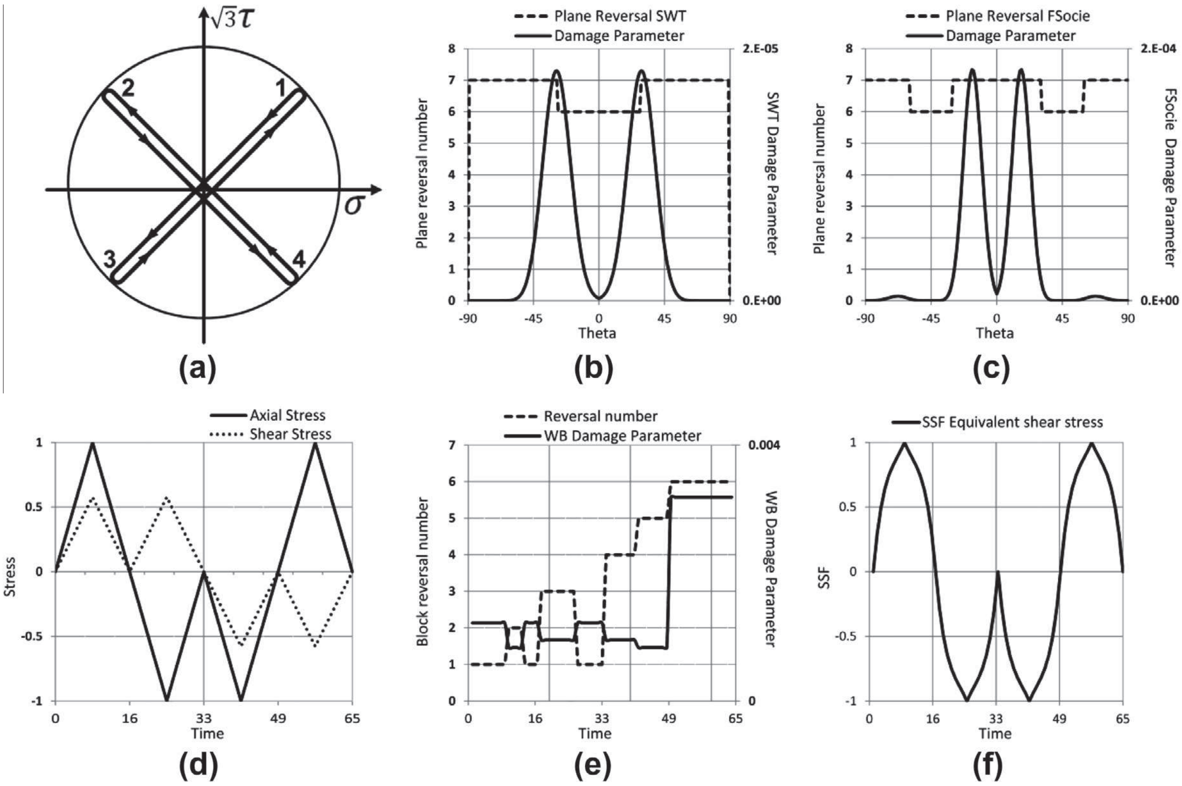

Fig. 8. Case 4: (a) von Mises stress space, (b) BS results with SWT, (c) BS results with F–Socie, (d) Block stress–time evolution, (e) WB results and (f) SSF time evolution.

based on the stress amplitude ratio (SAR) between shear and axial stress components. The block's SAR was 2, 0.5 and 0.6 in Cases 7–9, respectively.

In loading Cases 8 and 9, the axial stress amplitude is greater than the shear stress amplitude, i.e. axial damage predominates over shear one. In Case 7 the opposite occurs, i.e. the

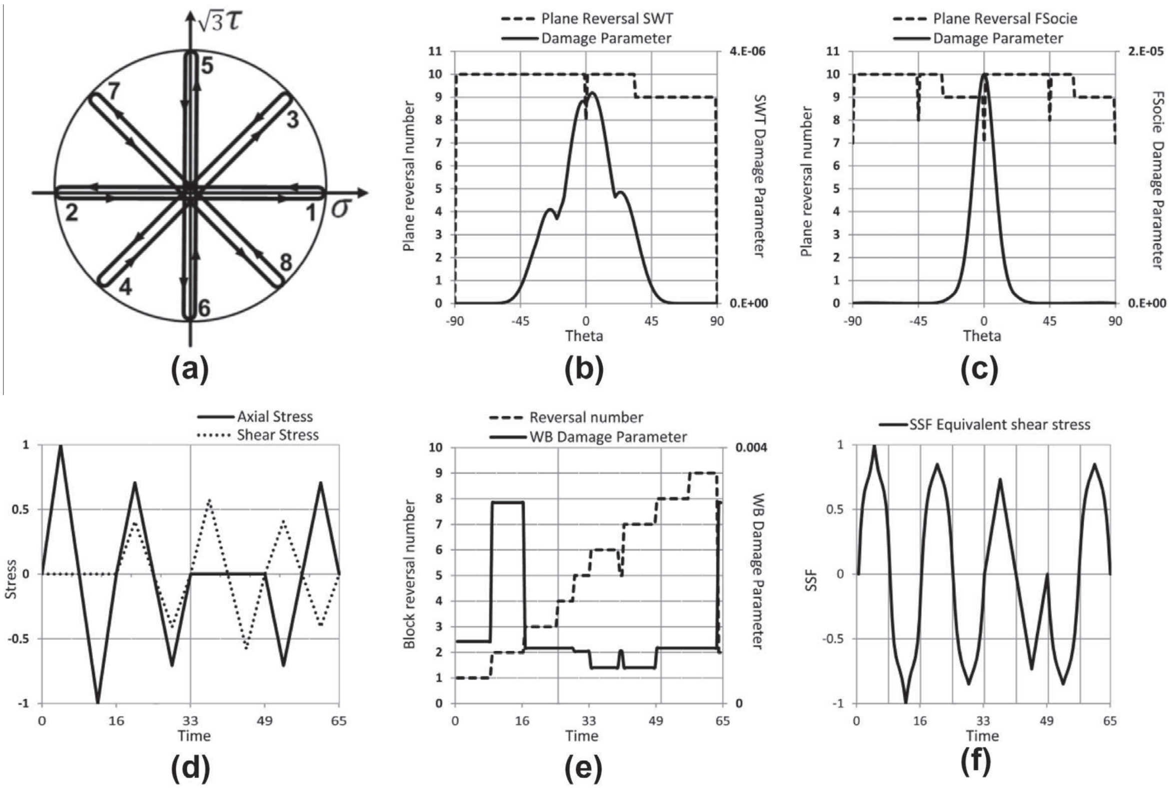

Fig. 9. Case 5: (a) von Mises stress space, (b) BS results with SWT, (c) BS results with F_Socie, (d) Block stress–time evolution, (e) WB results and (f) SSF time evolution.

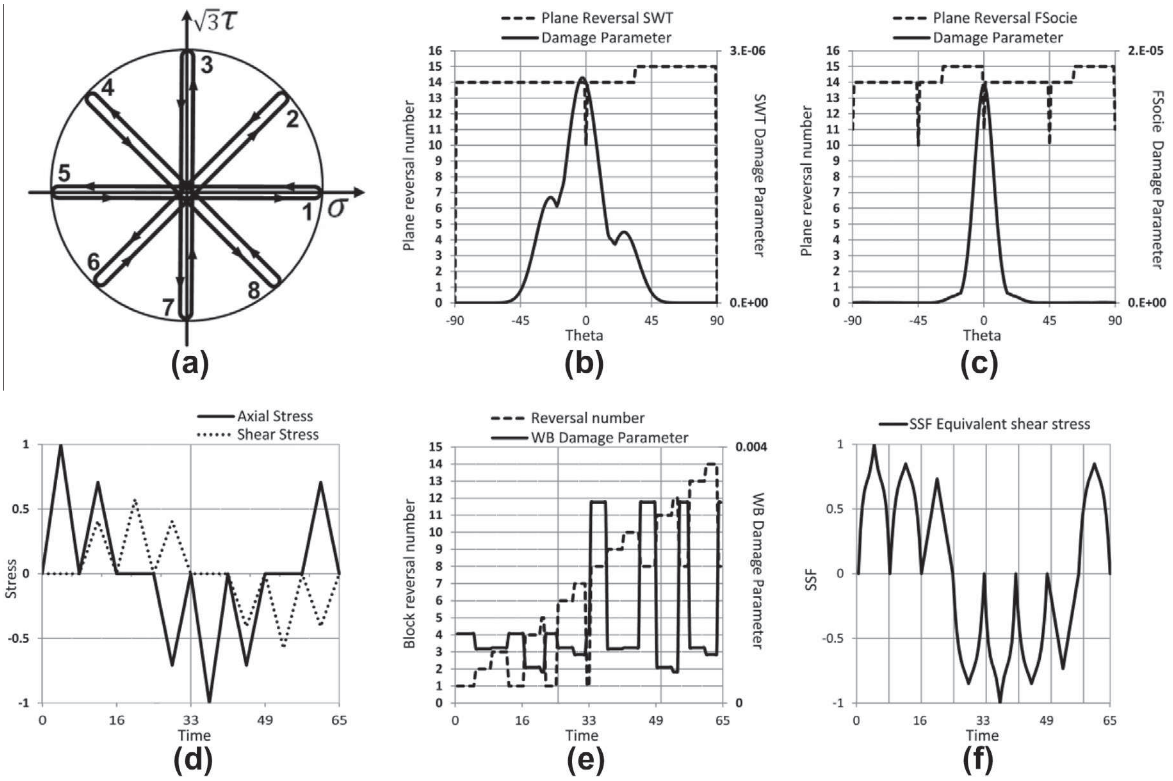

Fig. 10. Case 6: (a) von Mises stress space, (b) BS results with SWT, (c) BS results with F_Socie, (d) Block stress–time evolution, (e) WB results and (f) SSF time evolution.

shear damage predominates over the axial one. In this case, the shear stress amplitude is twice the axial one. Cases 8 and 9 have very similar results; therefore, little SAR variation causes little influence on reversals and accumulated damage results. Concerning Case 7 results, see Fig. 11, it can be concluded that SAR has a strong influence on the accumulated damage. However, BS criterion yields 11 reversals in the three asynchronous loading cases.

Please cite this article in press as: Anes V et al. New cycle counting method for multiaxial fatigue. Int J Fatigue (2014), http://dx.doi.org/10.1016/j.ijfatigue.2014.02.010

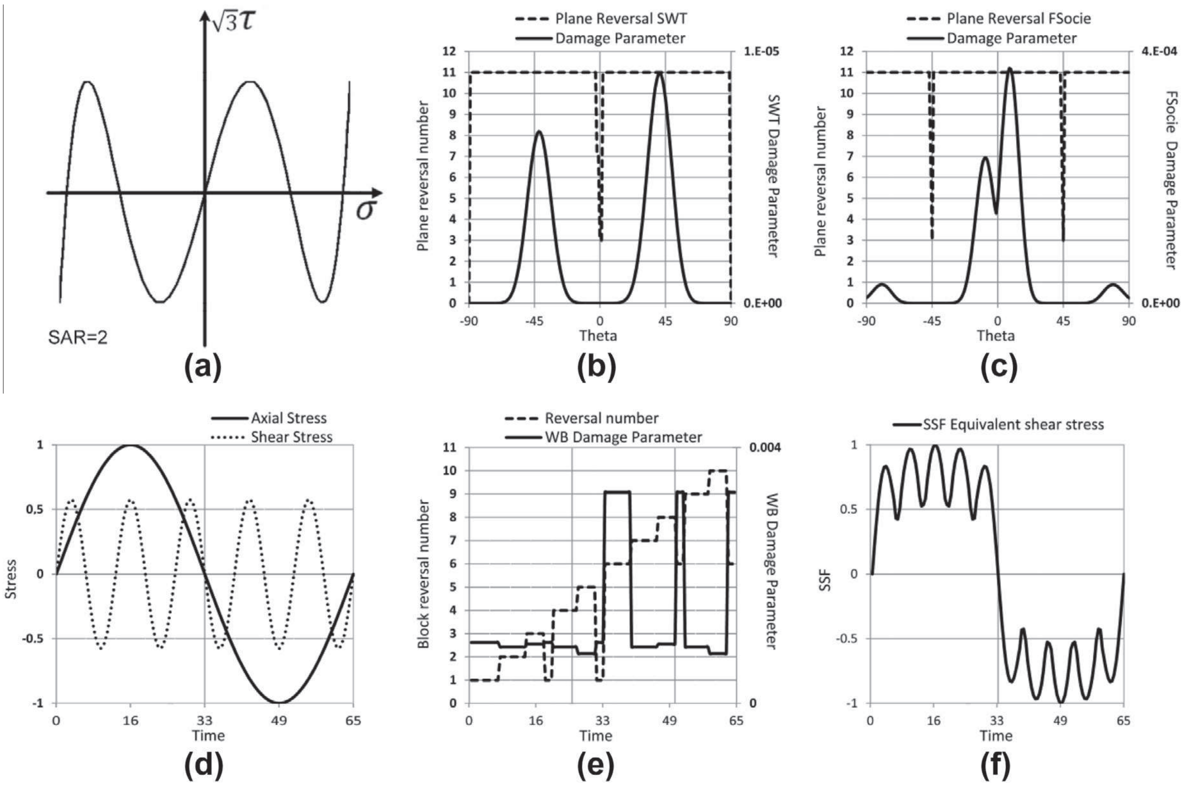

Fig. 11. Case 7: (a) von Mises stress space, (b) BS results with SWT, (c) BS results with F_Socie, (d) Block stress–time evolution, (e) WB results and (f) SSF time evolution.

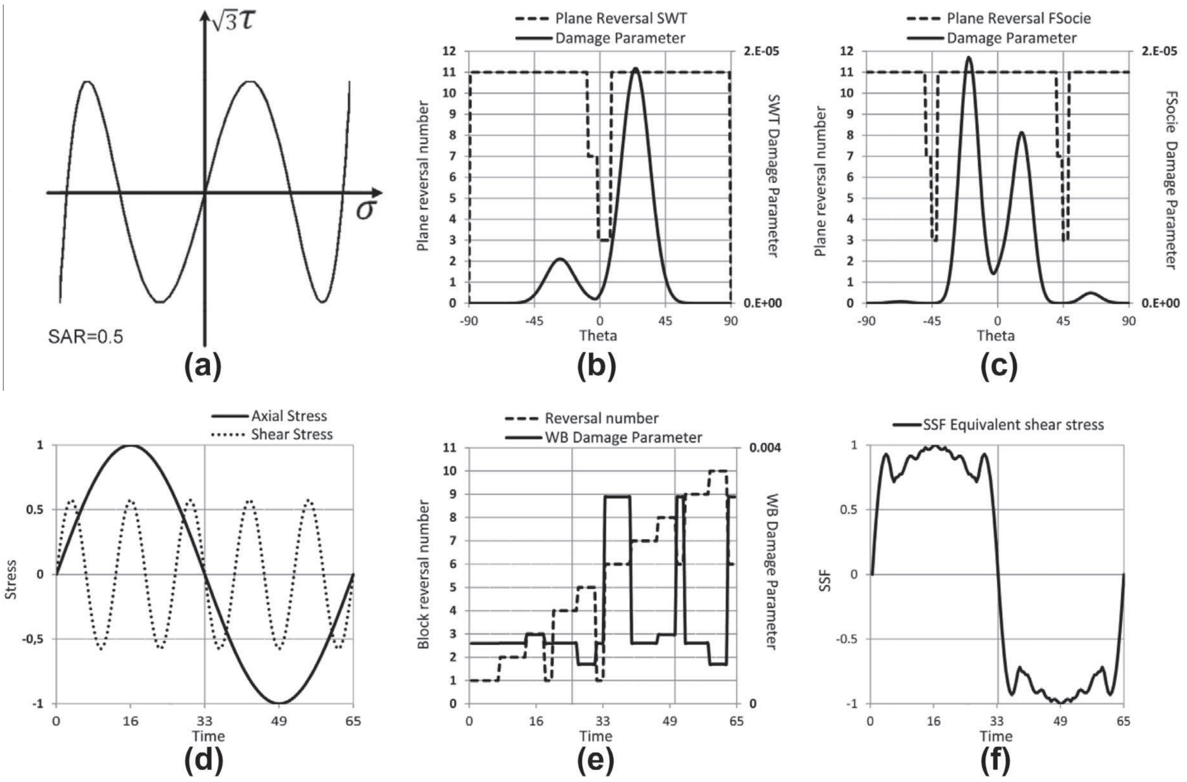

Fig. 12. Case 8: (a) von Mises stress space, (b) BS results with SWT, (c) BS results with F_Socie, (d) Block stress–time evolution, (e) WB results and (f) SSF time evolution.

Concerning loading Cases 8 and 9, BS model extracts 11 reversals in SWT and F–Socie critical plane criteria. Crack initiation estimations for Cases 8 and 9 were 24° and 26° in SWT and −20° and −19°, in F–Socie. Experimental results show −6° and −20° for crack initiation directions in Cases 8 and 9, respectively. Critical plane estimations without using a damage

Please cite this article in press as: Anes V et al. New cycle counting method for multiaxial fatigue. Int J Fatigue (2014), http://dx.doi.org/10.1016/j.ijfatigue.2014.02.010

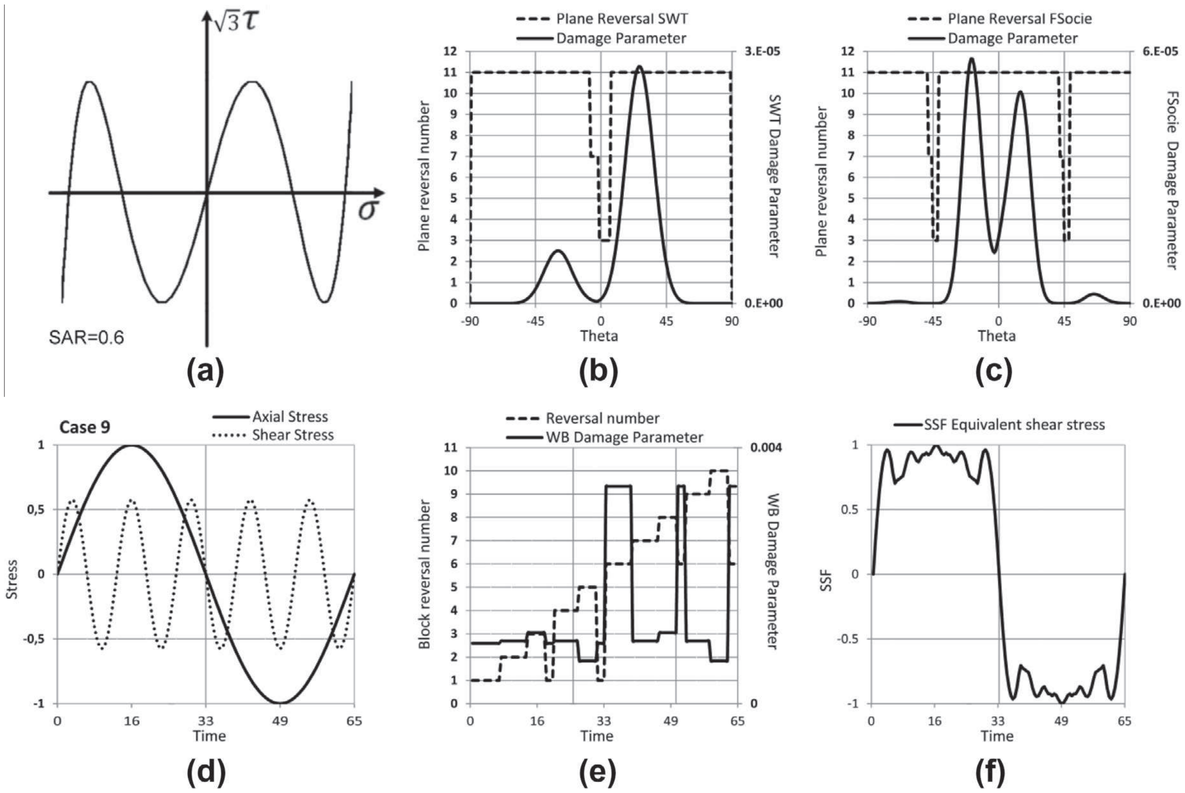

Fig. 13. Case 9: (a) von Mises stress space, (b) BS results with SWT, (c) BS results with F_Socie, (d) Block stress–time evolution, (e) WB results and (f) SSF time evolution.

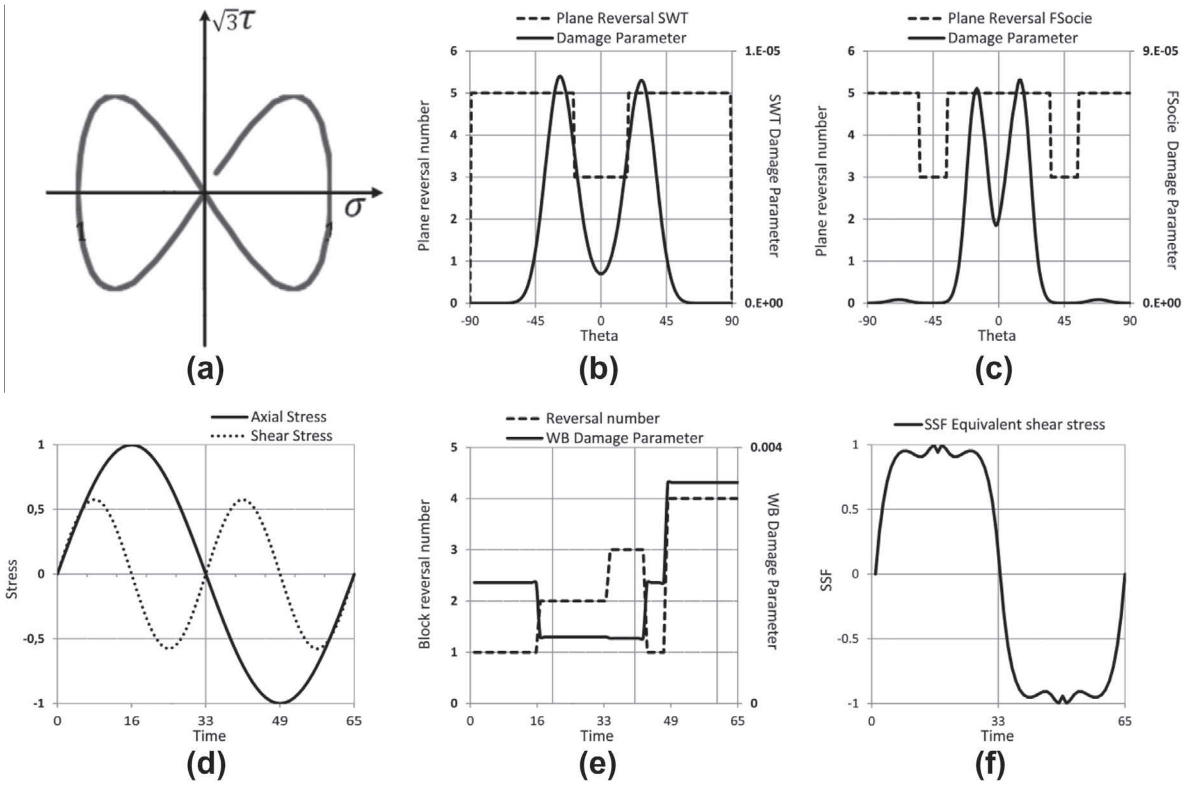

Fig. 14. Case 10: (a) von Mises stress space, (b) BS results with SWT, (c) BS results with F_Socie, (d) Block stress–time evolution, (e) WB results and (f) SSF time evolution.

accumulation criterion were, in Case 8, 0° in both SWT and F–Socie criteria.

Moreover, in Case 9, the critical plane estimation without accumulative damage criterion were −23/+25 for SWT, and −20/+70 for

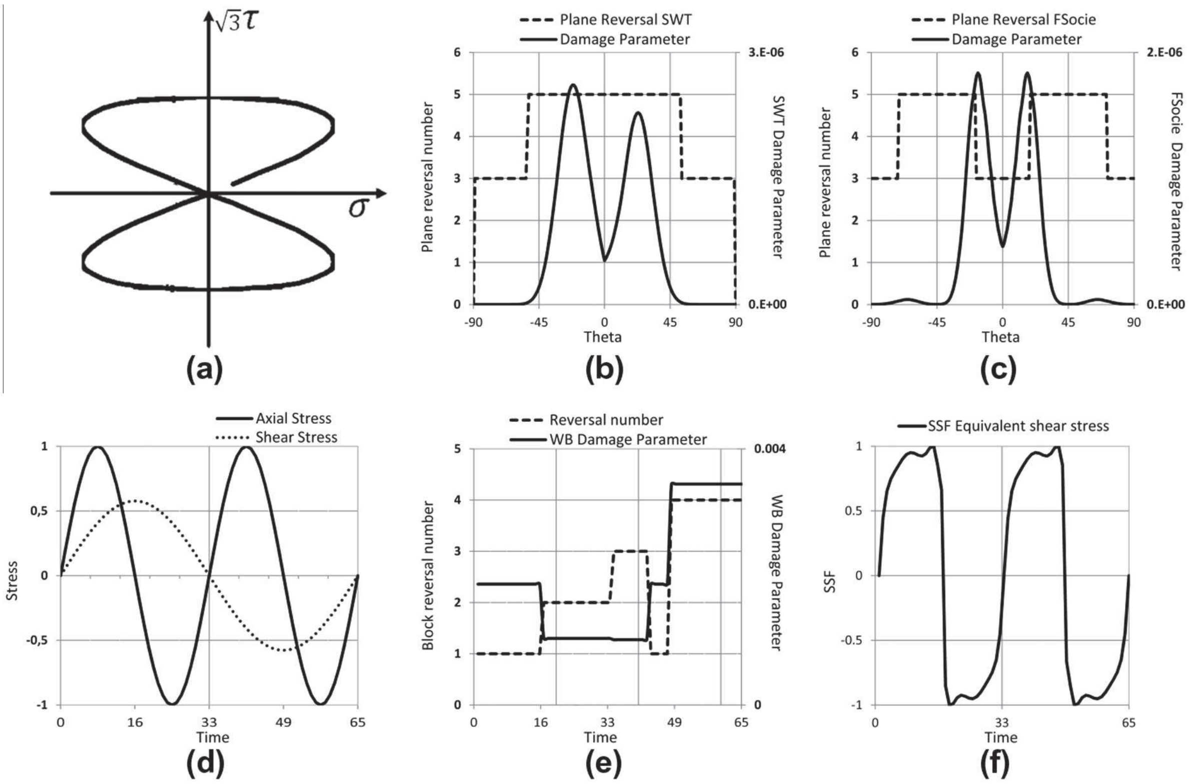

Fig. 15. Case 11: (a) von Mises stress space, (b) BS results with SWT, (c) BS results with F_Socie, (d) Block stress–time evolution, (e) WB results and (f) SSF time evolution.

F–Socie criterion. The critical plane estimation in loading Case 7 was 41° for SWT and 8° for the F–Socie criterion, respectively. The experimental crack initiation plane for loading Case 7 was −19°. Regarding Case 7, the critical plane direction without an accumulative damage approach were −39°; 38° in SWT and −13°; 12° in F–Socie. SSF reversals extraction from loading Cases 7–9 were 2, 1.8 and 1.8, respectively. Rainflow method applied to the SSF time variation yields 19, 27 and 27 reversals for Cases 7–9, respectively.

Loading Cases 10 and 11 results are summarized in Figs. 14 and 15. These loading blocks are asynchronous loadings where the shear stress frequency is twice the axial one in Case 10 and in Case 11 the axial stress frequency is twice the shear one. Concerning Case 10, BS criterion extracts 5 reversals in SWT and F–Socie at the most loaded plane (high accumulated damage). The critical plane estimation was −28° for SWT and 15° for F–Socie.

The Case 10 experimental crack direction was −18°. Critical plane estimations without an accumulative damage approach were ±25 in SWT and ±17/±73 in F–Socie. WB yields 4 reversals and the most damaging reversal was identified in the last quarter of the loading period. Regarding the results of the Case 11, the BS yields the same reversals amount achieved in Case 10, i.e. 5 reversals at the most loaded plane. Critical plane estimations under the BS accumulative approach were −22° in SWT and ±17° in F–Socie criterion. In Case 11 the experimental crack initiation direction was −23°. The critical estimations without an accumulative approach were ±21° in SWT and ±23/±67 in F–Socie criterion. WB extracts 4 reversals and the most damaging one occurs in the last quarter of the loading period.

Regarding the SSF reversals extraction from loading Cases 10 and 11 the results achieved were 1.8, and 1.5, respectively. Rainflow results from the SSF time variation yields 14 and 23 reversals in the loading Cases 10 and 11, respectively. Table 2 summarizes the critical plane estimations and critical plane experimental results from loading Cases 1–11.

Table 2
BS critical plane estimations and experimental results.

Case	SWT (°)	F–Socie (°)	BS–SWT (°)	BS–F-Socie (°)	Experiment (°)
1	0	±90; 0	0	0	−5
2	±45	±90; 0	±45	0	0
3	±25	±21; ±69	±30	±16	29
4	±25	±21; ±69	±29	±17	31
5	0	0	4	0	0
6	−25; 23	−23; 20	24	−20	−22
7	−39; 38	−13; 12	41	8	−19
8	0	0	−2	0	−6
9	−23; 25	−20; 70	26	−19	−20
10	±25	±17; ±73	−28	15	−18
11	±21	±23; ±67	−22	±17	−23

Table 3 summarizes the results from the Bannantine and Socie, Wang and Brown, SSF and Rainflow approaches. The results are presented in reversals, two reversals are equal to one cycle.

The BS cycle counting methodology aims to capture the damage behavior by using the rainflow method, a hysteresis loop method, to account block's reversals at each plane.

In contrast, WB criterion yields more or less damaging reversals within a loading block without any connectivity to the physical damage process.

It is not clear in the WB criterion why some regions of a loading block, i.e. reversals, are more damaging than other ones. However, BS and WB have similar results in the block's reversals extraction. The maximum difference between BS and WB reversals extraction was 3 in Case 8 and the minimum difference was 1 in several loading cases, see Table 3. SSF virtual cycle counting method in some loading cases extracts, from a loading block, a reversal quantity inferior to one, e.g. see Case 11 in Table 3. In Case 11 the SSF

Please cite this article in press as: Anes V et al. New cycle counting method for multiaxial fatigue. Int J Fatigue (2014), http://dx.doi.org/10.1016/j.ijfatigue.2014.02.010

Table 3
Cycle counting results for Bannantine and Socie, Wang and Brown, SSF virtual cycle counting and rainflow methods, results given in reversals.

Case	BS–SWT	BS–F–Socie	WB	SSF	SSF–Rainflow
1	4	3	4	3.4	5
2	5	3	4	3.7	5
3	7	7	6	4.1	5
4	6	7	6	4.0	6
5	10	7	9	6.9	10
6	11	11	10	1.9	14
7	11	11	10	2.0	19
8	14	11	14	6.8	27
9	11	11	10	1.8	27
10	5	5	4	1.8	14
11	5	3	3	1.4	23

method extracts 1.4 reversals, which is one reversal plus 40% from another one. To explain this result must be recalled the SSF virtual cycle counting paradigm, where the sum of the absolute values of peaks and valleys divided by two times the maximum peak yields the block's damage. The relative block's damage indicates how many times a loading block is more damaging than the reference one used to set up SN curves, e.g. sinusoidal $R = -1$. Therefore, the SSF virtual cycle counting yields a non-integer reversal sum. The SSF cycles extraction amount was inferior to the ones obtained with BS and WB Brown criteria.

4.3. Fatigue life correlation

In order to estimate the block's fatigue life, it was used the reversals extracted in each cycle counting criterion coupled with a damage parameter and with the Miner's rule.

Fig. 16 shows the fatigue life correlation between theoretical estimations and experimental results for BS criterion in association with a critical plane model.

Sub-figures a and b show the BS–SWT results and sub-figures c and d show the BS- F–Socie results. BS–SWT criterion yields an accumulative damage parameter too low because the correlation tends to be above the boundary line.

Regarding the F–Socie results, the correlation yields an inconclusive trend in loading Cases 1–6 where can be found a big scatter. In contrast, for Cases 7–11, F–Socie fatigue life correlation yields very acceptable results with only two points outside of the boundary lines.

The Wang and Brown fatigue life correlation is presented in Fig. 17. Sub-figures a and b show the fatigue life results for $S = 0.3$, which sets up the Wang and Brown damage parameter to the infinite fatigue life estimations, and sub-figures c and d) shows the fatigue life correlation for half fatigue life estimations with $S = 0.7$. Likewise the BS results, loading Cases 1–6 show a big scatter for $S = 0.3$ and $S = 0.7$ and it can be seen that the accumulative damage parameter is too high in loading Cases 1–6.

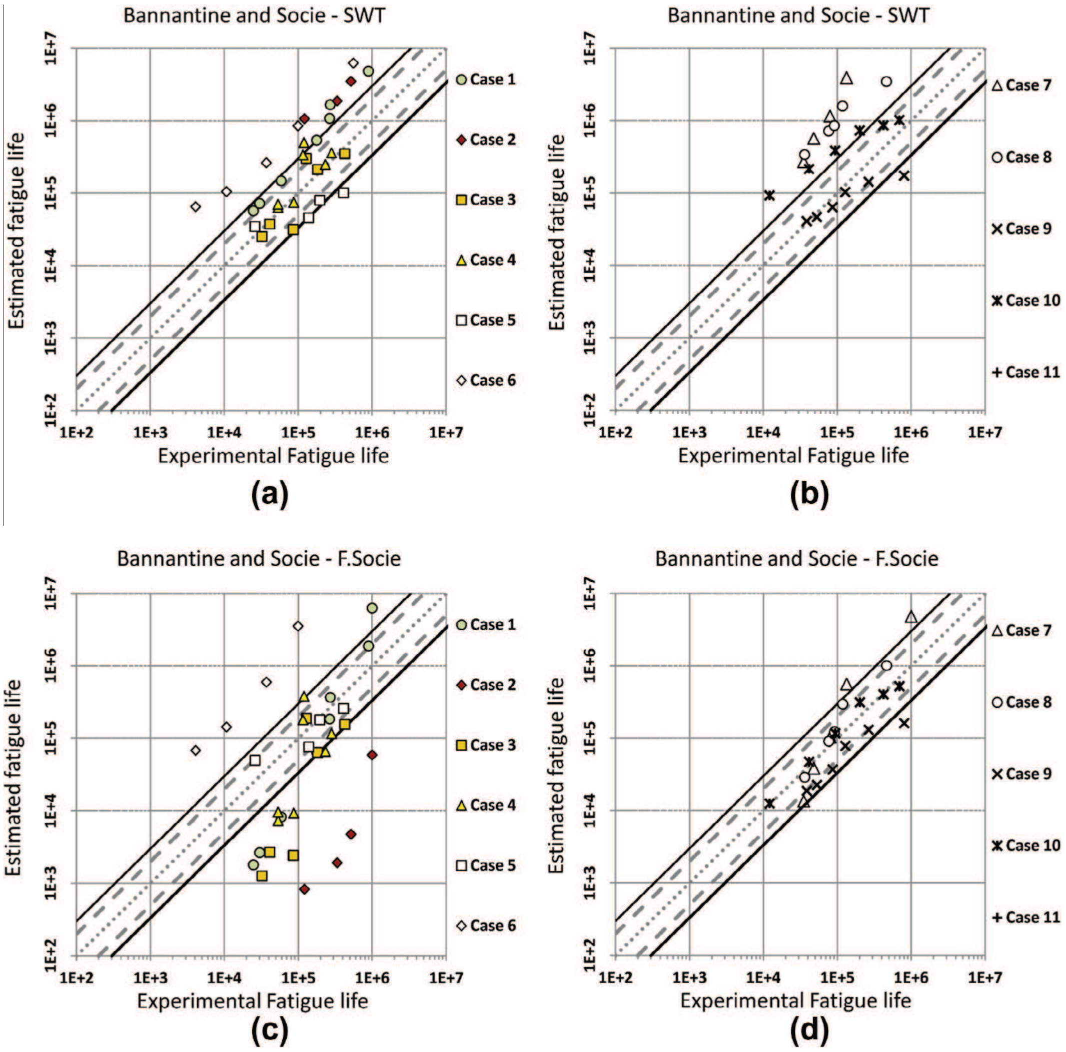

Fig. 16. Fatigue life correlation for BS–SWT (a and b) and for BS-FSocie and (c and d) criteria.

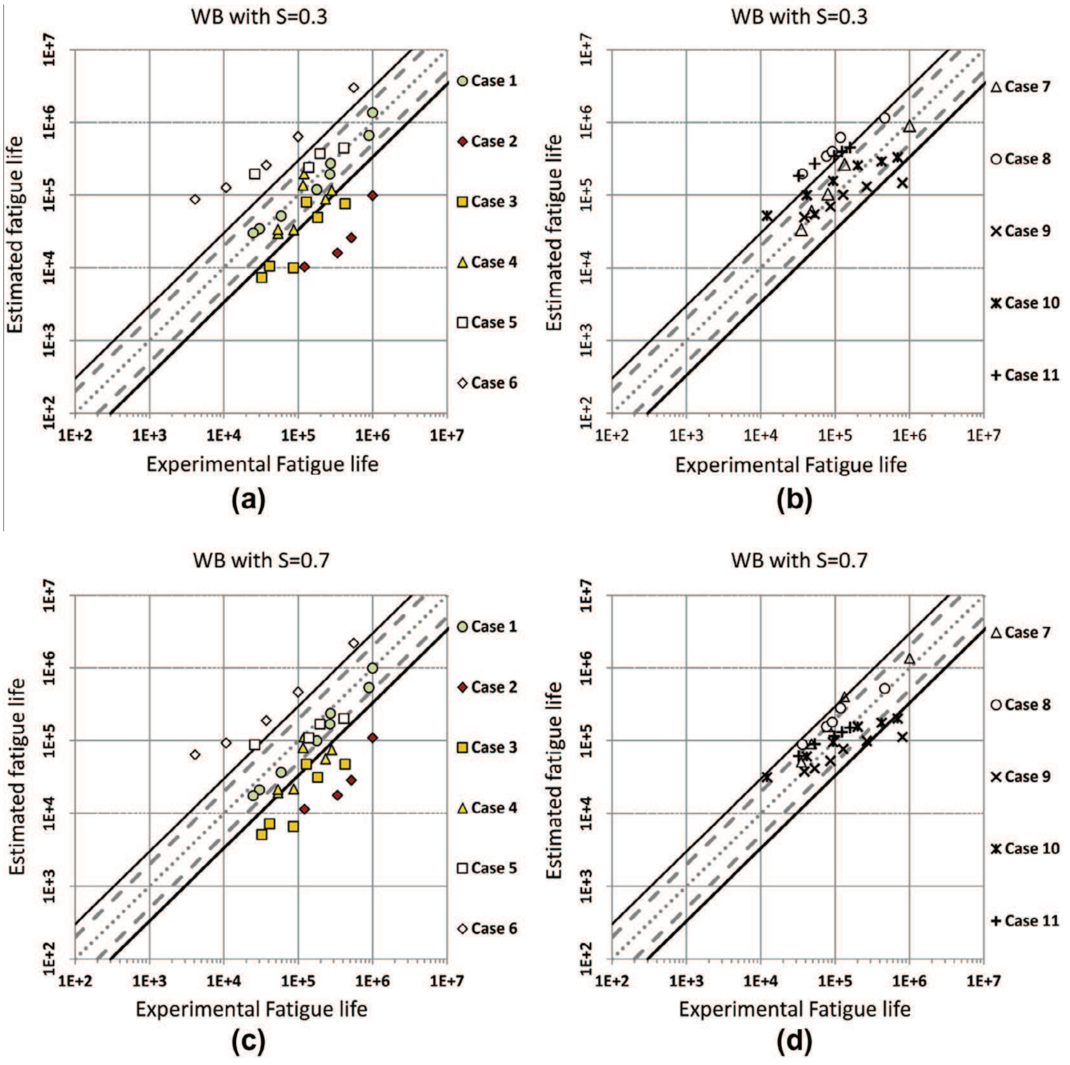

Fig. 17. Fatigue life correlation for WB with $S = 0.3$ (a and b) and (c and d) with $S = 0.7$.

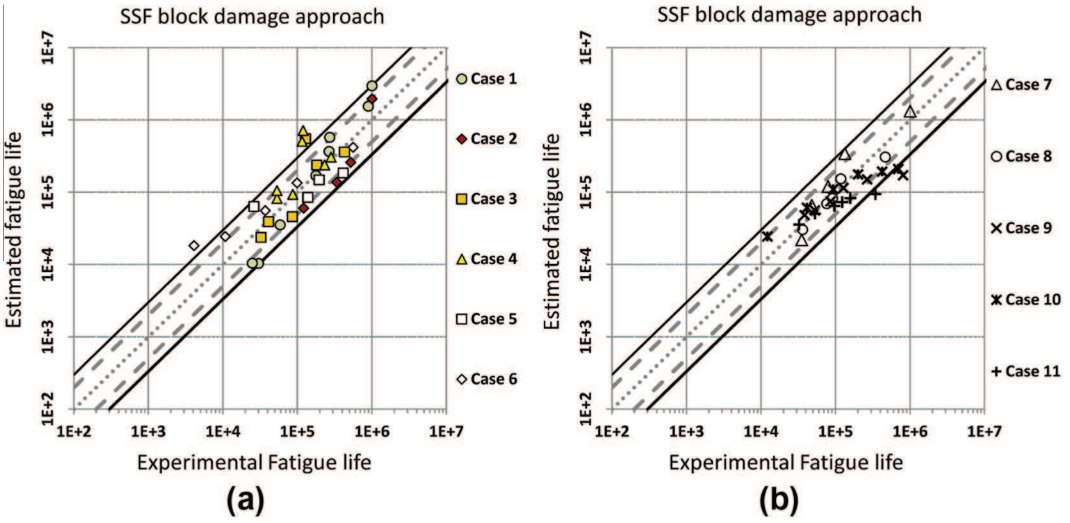

Fig. 18. (a and b) Fatigue life correlation for the SSF virtual cycle counting in association with the SSF equivalent shear stress.

Nevertheless, for Cases 7–11, a better correlation with very acceptable results was achieved with $S = 0.7$, likewise observed in BS criterion.

Fig. 18 shows the proposed models fatigue correlation with experimental results where the scatter shown in BS and WB fatigue life correlations at Cases 1–6 was reduced.

Please cite this article in press as: Anes V et al. New cycle counting method for multiaxial fatigue. Int J Fatigue (2014), http://dx.doi.org/10.1016/j.ijfatigue.2014.02.010

Moreover, the results for loading Cases 7–11 are within the fatigue life boundary with only 2 experimental results outside.

Therefore, the proposed SSF virtual cycle counting method coupled with the new fatigue life criterion yields improved results in loading block's fatigue life estimations.

Moreover, the new proposals have the advantage to be a very simple and quick method to estimate a loading block fatigue life. The complexity involved in the BS and WB reversals extraction leads to conclude that these cycle counting methodologies are not very practical to implement manually or even in a numeric code.

5. Conclusions

In this paper, one method and one criterion are proposed in order to characterize multiaxial fatigue under complex loading blocks.

The proposed cycle counting method, the SSF virtual cycle counting, was implemented to extract the loading reversals within a multiaxial loading block and it is based in the SSF equivalent shear stress.

The multiaxial criterion was implemented to estimate multiaxial fatigue life under loading block conditions and it is based on the SSF virtual cycle counting method. In order to validate the proposed criterion it was carried out eleven loading blocks with different loading effects.

Moreover, fatigue life correlations based in two multiaxial cycle counting methods, the Bannatine and Socie and the Wang and Brown, were compared with the new criterion fatigue life estimations.

Results show that the proposed fatigue life criterion was successfully validated. Moreover, the proposed criterion has better fatigue life correlations than the ones achieved by the Bannatine and Socie and the Wang and Brown criteria. Furthermore, it should be underlined the simplicity to implement the new cycle counting method and the new fatigue life criterion.

Acknowledgement

The authors gratefully acknowledge financial support from FCT – Fundação para Ciência e Tecnologia (Portuguese Foundation for Science and Technology), through the Project PTDC/EME-PME/104404/2008.

Appendix A. Supplementary material

Supplementary material associated with this article can be found, in the online version, at http://dx.doi.org/10.1016/j.ijfatigue.2014.02.010.

References

[1] Miner MA. Cumulative damage in fatigue. J Appl Mech 1945;12:159–64.
[2] Socie DF, Marquis GB. Multiaxial fatigue. PA: Society of Automotive Engineers Warrendale; 2000.
[3] Carpinteri A, Spagnoli A, Vantadori S, Bagni C. Structural integrity assessment of metallic components under multiaxial fatigue: the C–S criterion and its evolution. Fatigue Fract Eng Mater Struct 2013:1–14.
[4] Carpinteri A, Spagnoli A. Multiaxial high-cycle fatigue criterion for hard metals. Int J Fatigue 2001;23:135–45.
[5] Brighenti R, Carpinteri A. A notch multiaxial-fatigue approach based on damage mechanics. Int J Fatigue 2012;39:122–33.
[6] Meggiolaro MA, de Castro JTP. An improved multiaxial rainflow algorithm for non-proportional stress or strain histories – Part II: The modified Wang–Brown method. Int J Fatigue 2012;42:194–206.
[7] Meggiolaro MA, de Castro JTP. An improved multiaxial rainflow algorithm for non-proportional stress or strain histories – Part I: Enclosing surface methods. Int J Fatigue 2012;42:217–26.
[8] Wei Z, Dong P. Multiaxial fatigue life assessment of welded structures. Eng Fract Mech 2010;77:3011–21.
[9] Langlais TE, Vogel JH, Chase TR. Multiaxial cycle counting for critical plane methods. Int J Fatigue 2003;25:641–7.
[10] Chen H, Shang DG, Liu ET. Multiaxial fatigue life prediction method based on path-dependent cycle counting under tension/torsion random loading. Fatigue Fract Eng Mater Struct 2011;34:782–91.
[11] A. International, E-1049. Standard practices for cycle counting in fatigue analysis, Philadelphia, 2005.
[12] Wei Z, Dong P. A rapid path-length searching procedure for multi-axial fatigue cycle counting. Fatigue Fract Eng Mater Struct 2012;35:556–71.
[13] Dong P, Wei Z, Hong JK. A path-dependent cycle counting method for variable-amplitude multi-axial loading. Int J Fatigue 2010;32:720–34.
[14] Wang CH, Brown MW. A path-independent parameter for fatigue under proportional and non-proportional loading. Fatigue Fract Eng Mater Struct 1993;16:1285–97.
[15] Anes V, Reis L, Li B, Fonte M, de Freitas M. New approach for analysis of complex multiaxial loading paths. Int J Fatigue 2013.
[16] Musallam M, Johnson CM. An efficient implementation of the rainflow counting algorithm for life consumption estimation. IEEE Transactions on reliability 2012;61:978–86.
[17] McInnes CH, Meehan PA. Equivalence of four-point and three-point rainflow cycle counting algorithms. Int J Fatigue 2008;30:547–59.
[18] Colombi P, Dolinski K. Fatigue lifetime of welded joints under random loading: rainflow cycle vs. cycle sequence method. Probab Eng Mech 2001;16:61–71.
[19] Anthes RJ. Modified rainflow counting keeping the load sequence. Int J Fatigue 1997;19:529–35.
[20] You B-R, Lee S-B. A critical review on multiaxial fatigue assessments of metals. Int J Fatigue 1996;18:235–44.
[21] Matsuishi M, Endo T. Fatigue of metals subjected to varying stress. Fukuoka, Japan: Japan Society of Mechanical Engineers; 1968. p. 37–40.
[22] Downing SD, Socie DF. Simple rainflow counting algorithms. Int J Fatigue 1982;4:31–40.
[23] Fatemi A, Yang L. Cumulative fatigue damage and life prediction theories: a survey of the state of the art for homogeneous materials. Int J Fatigue 1998;20:9–34.
[24] Wang CH, Brown MW. On plastic deformation and fatigue under multiaxial loading. Int J Fatigue 1997;19. 661–661.